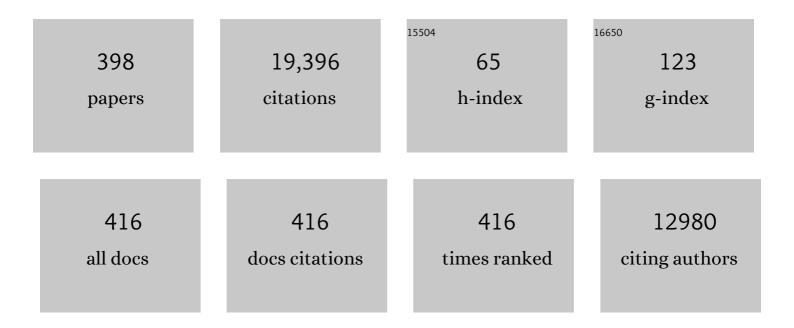
Daniel Jaque

List of Publications by Year in descending order

Source: https://exaly.com/author-pdf/3939744/publications.pdf Version: 2024-02-01



#	Article	IF	CITATIONS
1	Nanoparticles for photothermal therapies. Nanoscale, 2014, 6, 9494-9530.	5.6	1,562
2	Temperature Sensing Using Fluorescent Nanothermometers. ACS Nano, 2010, 4, 3254-3258.	14.6	1,284
3	Luminescence nanothermometry. Nanoscale, 2012, 4, 4301.	5.6	1,214
4	NIR-to-NIR Two-Photon Excited CaF ₂ :Tm ³⁺ ,Yb ³⁺ Nanoparticles: Multifunctional Nanoprobes for Highly Penetrating Fluorescence Bio-Imaging. ACS Nano, 2011, 5, 8665-8671.	14.6	381
5	Subtissue Thermal Sensing Based on Neodymium-Doped LaF ₃ Nanoparticles. ACS Nano, 2013, 7, 1188-1199.	14.6	338
6	Advances and challenges for fluorescence nanothermometry. Nature Methods, 2020, 17, 967-980.	19.0	333
7	CdSe Quantum Dots for Two-Photon Fluorescence Thermal Imaging. Nano Letters, 2010, 10, 5109-5115.	9.1	276
8	Intratumoral Thermal Reading During Photoâ€Thermal Therapy by Multifunctional Fluorescent Nanoparticles. Advanced Functional Materials, 2015, 25, 615-626.	14.9	274
9	Properties of Nd^3+-doped and undoped tetragonal PbWO_4, NaY(WO_4)_2, CaWO_4, and undoped monoclinic ZnWO_4 and CdWO_4 as laser-active and stimulated Raman scattering-active crystals. Applied Optics, 1999, 38, 4533.	2.1	270
10	Unveiling in Vivo Subcutaneous Thermal Dynamics by Infrared Luminescent Nanothermometers. Nano Letters, 2016, 16, 1695-1703.	9.1	265
11	In Vivo Luminescence Nanothermometry: from Materials to Applications. Advanced Optical Materials, 2017, 5, 1600508.	7.3	258
12	Nd:YAG Nearâ€infrared Luminescent Nanothermometers. Advanced Optical Materials, 2015, 3, 687-694.	7.3	256
13	Standardizing luminescence nanothermometry for biomedical applications. Nanoscale, 2020, 12, 14405-14421.	5.6	241
14	Neodymiumâ€Doped LaF ₃ Nanoparticles for Fluorescence Bioimaging in the Second Biological Window. Small, 2014, 10, 1141-1154.	10.0	185
15	1.3 \hat{l} /4m emitting SrF2:Nd3+ nanoparticles for high contrast in vivo imaging in the second biological window. Nano Research, 2015, 8, 649-665.	10.4	185
16	Intracellular imaging of HeLa cells by non-functionalized NaYF4 : Er ³⁺ , Yb ³⁺ upconverting nanoparticles. Nanoscale, 2010, 2, 495-498.	5.6	179
17	Inorganic nanoparticles for optical bioimaging. Advances in Optics and Photonics, 2016, 8, 1.	25.5	175
18	Hybrid Nanostructures for High‣ensitivity Luminescence Nanothermometry in the Second Biological Window. Advanced Materials, 2015, 27, 4781-4787.	21.0	174

#	Article	IF	CITATIONS
19	In Vivo Subcutaneous Thermal Video Recording by Supersensitive Infrared Nanothermometers. Advanced Functional Materials, 2017, 27, 1702249.	14.9	159
20	Highly efficient laser action in femtosecond-written Nd:yttrium aluminum garnet ceramic waveguides. Applied Physics Letters, 2008, 92, .	3.3	150
21	Refractive index change mechanisms in femtosecond laser written ceramic Nd:YAG waveguides: micro-spectroscopy experiments and beam propagation calculations. Applied Physics B: Lasers and Optics, 2009, 95, 85-96.	2.2	141
22	Lifetime-Encoded Infrared-Emitting Nanoparticles for <i>in Vivo</i> Multiplexed Imaging. ACS Nano, 2018, 12, 4362-4368.	14.6	138
23	Er:Yb:NaY ₂ F ₅ O up-converting nanoparticles for sub-tissue fluorescence lifetime thermal sensing. Nanoscale, 2014, 6, 9727.	5.6	131
24	Highâ€ S ensitivity Fluorescence Lifetime Thermal Sensing Based on CdTe Quantum Dots. Small, 2012, 8, 2652-2658.	10.0	130
25	Thermal Scanning at the Cellular Level by an Optically Trapped Upconverting Fluorescent Particle. Advanced Materials, 2016, 28, 2421-2426.	21.0	128
26	CdTe Quantum Dots as Nanothermometers: Towards Highly Sensitive Thermal Imaging. Small, 2011, 7, 1774-1778.	10.0	127
27	Reliability of rare-earth-doped infrared luminescent nanothermometers. Nanoscale, 2018, 10, 22319-22328.	5.6	124
28	Red, green, and blue laser light from a single Nd:YAl3(BO3)4 crystal based on laser oscillation at 1.3 μm. Applied Physics Letters, 1999, 75, 325-327.	3.3	121
29	Yb3+/Tm3+ co-doped NaNbO3 nanocrystals as three-photon-excited luminescent nanothermometers. Sensors and Actuators B: Chemical, 2015, 213, 65-71.	7.8	120
30	Fluorescent nanothermometers for intracellular thermal sensing. Nanomedicine, 2014, 9, 1047-1062.	3.3	117
31	Infraredâ€Emitting QDs for Thermal Therapy with Realâ€Time Subcutaneous Temperature Feedback. Advanced Functional Materials, 2016, 26, 6060-6068.	14.9	117
32	Nd3+ doped LaF3 nanoparticles as self-monitored photo-thermal agents. Applied Physics Letters, 2014, 104, 053703.	3.3	116
33	Ag/Ag ₂ S Nanocrystals for High Sensitivity Nearâ€Infrared Luminescence Nanothermometry. Advanced Functional Materials, 2017, 27, 1604629.	14.9	110
34	PbS/CdS/ZnS Quantum Dots: A Multifunctional Platform for In Vivo Nearâ€Infrared Lowâ€Dose Fluorescence Imaging. Advanced Functional Materials, 2015, 25, 6650-6659.	14.9	108
35	Overcoming Autofluorescence: Longâ€Lifetime Infrared Nanoparticles for Timeâ€Gated In Vivo Imaging. Advanced Materials, 2016, 28, 10188-10193.	21.0	108
36	Self-monitored photothermal nanoparticles based on core–shell engineering. Nanoscale, 2016, 8, 3057-3066.	5.6	107

#	Article	IF	CITATIONS
37	Heating efficiency of multi-walled carbon nanotubes in the first and second biological windows. Nanoscale, 2013, 5, 7882.	5.6	106
38	Neodymium-doped nanoparticles for infrared fluorescence bioimaging: The role of the host. Journal of Applied Physics, 2015, 118, .	2.5	102
39	Optical bands and energy levels of ion in the nonlinear laser crystal. Journal of Physics Condensed Matter, 1997, 9, 9715-9729.	1.8	100
40	Bio-functionalization of ligand-free upconverting lanthanide doped nanoparticles for bio-imaging and cell targeting. Nanoscale, 2012, 4, 3647.	5.6	94
41	Doping Lanthanide Ions in Colloidal Semiconductor Nanocrystals for Brighter Photoluminescence. Chemical Reviews, 2021, 121, 1425-1462.	47.7	94
42	Water (H ₂ O and D ₂ O) Dispersible NIR-to-NIR Upconverting Yb ³⁺ /Tm ³⁺ Doped MF ₂ (M = Ca, Sr) Colloids: Influence of the Host Crystal. Crystal Growth and Design, 2013, 13, 4906-4913.	3.0	93
43	Growth, spectroscopic, and laser properties of Yb^3+-doped Lu_3Al_5O_12 garnet crystal. Journal of the Optical Society of America B: Optical Physics, 2006, 23, 676.	2.1	92
44	<i>In vivo</i> autofluorescence in the biological windows: the role of pigmentation. Journal of Biophotonics, 2016, 9, 1059-1067.	2.3	90
45	Nd3+→Yb3+energy transfer in theYAl3(BO3)4nonlinear laser crystal. Physical Review B, 2003, 68, .	3.2	89
46	Energy transfer with migration. Generalization of the Yokota–Tanimoto model for any kind of multipole interaction. Journal of Chemical Physics, 1999, 111, 1191-1194.	3.0	87
47	Rare-earth-doped fluoride nanoparticles with engineered long luminescence lifetime for time-gated <i>in vivo</i> optical imaging in the second biological window. Nanoscale, 2018, 10, 17771-17780.	5.6	87
48	Quantum Dot Thermometry Evaluation of Geometry Dependent Heating Efficiency in Gold Nanoparticles. Langmuir, 2014, 30, 1650-1658.	3.5	85
49	Deep tissue bio-imaging using two-photon excited CdTe fluorescent quantum dots working within the biological window. Nanoscale, 2012, 4, 298-302.	5.6	84
50	Accurate In Vivo Nanothermometry through NIRâ€I Lanthanide Luminescence Lifetime. Small, 2020, 16, e2004118.	10.0	84
51	Luminescence based temperature bio-imaging: Status, challenges, and perspectives. Applied Physics Reviews, 2021, 8, .	11.3	84
52	In Vivo Early Tumor Detection and Diagnosis by Infrared Luminescence Transient Nanothermometry. Advanced Functional Materials, 2018, 28, 1803924.	14.9	83
53	Femtosecond laser inscribed cladding waveguides in Nd:YAG ceramics: Fabrication, fluorescence imaging and laser performance. Optics Express, 2012, 20, 18620.	3.4	82
54	<i>In Vivo</i> Spectral Distortions of Infrared Luminescent Nanothermometers Compromise Their Reliability. ACS Nano, 2020, 14, 4122-4133.	14.6	82

#	Article	IF	CITATIONS
55	70% slope efficiency from an ultrafast laser-written Nd:GdVO_4 channel waveguide laser. Optics Express, 2010, 18, 24994.	3.4	80
56	LaF3 core/shell nanoparticles for subcutaneous heating and thermal sensing in the second biological-window. Applied Physics Letters, 2016, 108, .	3.3	78
57	In Vivo Contactless Brain Nanothermometry. Advanced Functional Materials, 2018, 28, 1806088.	14.9	78
58	Nanoparticles for highly efficient multiphoton fluorescence bioimaging. Optics Express, 2010, 18, 23544.	3.4	77
59	Neodymiumâ€Based Stoichiometric Ultrasmall Nanoparticles for Multifunctional Deepâ€Tissue Photothermal Therapy. Advanced Optical Materials, 2016, 4, 782-789.	7.3	73
60	In Vivo Ischemia Detection by Luminescent Nanothermometers. Advanced Healthcare Materials, 2017, 6, 1601195.	7.6	73
61	Ag ₂ S Nanoheaters with Multiparameter Sensing for Reliable Thermal Feedback during In Vivo Tumor Therapy. Advanced Functional Materials, 2020, 30, 2002730.	14.9	73
62	Real-time deep-tissue thermal sensing with sub-degree resolution by thermally improved Nd3+:LaF3 multifunctional nanoparticles. Journal of Luminescence, 2016, 175, 149-157.	3.1	71
63	Optical Torques on Upconverting Particles for Intracellular Microrheometry. Nano Letters, 2016, 16, 8005-8014.	9.1	70
64	Perspectives for Ag ₂ S NIR-II nanoparticles in biomedicine: from imaging to multifunctionality. Nanoscale, 2019, 11, 19251-19264.	5.6	69
65	Diffuse multiself-frequency conversion processes in the blue and green by quasicylindrical ferroelectric domains in Nd3+:Sr0.6Ba0.4(NbO3)2 laser crystal. Applied Physics Letters, 2001, 78, 1961-1963.	3.3	68
66	Coherent Light Generation from aNdâ^¶SBNNonlinear Laser Crystal through its Ferroelectric Phase Transition. Physical Review Letters, 2005, 95, 267401.	7.8	67
67	Quantum Dotâ€Based Thermal Spectroscopy and Imaging of Optically Trapped Microspheres and Single Cells. Small, 2013, 9, 2162-2170.	10.0	67
68	Optical trapping of NaYF4:Er3+,Yb3+ upconverting fluorescent nanoparticles. Nanoscale, 2013, 5, 12192.	5.6	66
69	Comparison of optical spectra of Nd3+in NdAl3(BO3)4(NAB), Nd:GdAl3(BO3)4(NGAB) and Nd:Gd0.2Y0.8Al3(BO3)4(NGYAB) crystals. Journal of Physics Condensed Matter, 2001, 13, 1171-1178.	1.8	65
70	Upconverting Nanoparticle to Quantum Dot Förster Resonance Energy Transfer: Increasing the Efficiency through Donor Design. ACS Photonics, 2018, 5, 2261-2270.	6.6	63
71	Core–shell rare-earth-doped nanostructures in biomedicine. Nanoscale, 2018, 10, 12935-12956.	5.6	63
72	Upconversion nanoparticles for <i>in vivo</i> applications: limitations and future perspectives. Methods and Applications in Eluorescence, 2019, 7, 022001	2.3	63

#	Article	IF	CITATIONS
73	Blue-light laser source by sum-frequency mixing in Nd:YAl3(BO3)4. Applied Physics Letters, 1998, 73, 3659-3661.	3.3	62
74	Continuous-wave laser properties of the self-frequency-doubling YAl_3(BO_3)_4: Nd crystal. Journal of the Optical Society of America B: Optical Physics, 1998, 15, 1656.	2.1	61
75	lon migration assisted inscription of high refractive index contrast waveguides by femtosecond laser pulses in phosphate glass. Optics Letters, 2013, 38, 5248.	3.3	61
76	Upconverting nanocomposites with combined photothermal and photodynamic effects. Nanoscale, 2018, 10, 791-799.	5.6	61
77	Continuous wave laser radiation at 524 nm from a self-frequency-doubled laser of LaBGeO5:Nd3+. Applied Physics Letters, 1998, 72, 531-533.	3.3	60
78	Nanosecond Nd ³⁺ :LuVO ₄ self-Raman laser. Laser Physics Letters, 2009, 6, 374-379.	1.4	60
79	Luminescent nanoprobes for thermal bio-sensing: Towards controlled photo-thermal therapies. Journal of Luminescence, 2016, 169, 394-399.	3.1	59
80	Nd 3+ ions in nanomedicine: Perspectives and applications. Optical Materials, 2017, 63, 185-196.	3.6	59
81	Optomagnetic Nanoplatforms for In Situ Controlled Hyperthermia. Advanced Functional Materials, 2018, 28, 1704434.	14.9	59
82	Rare earth and transition metal ion centers in LiNbO3. Spectrochimica Acta - Part A: Molecular and Biomolecular Spectroscopy, 1998, 54, 1571-1581.	3.9	57
83	Optical characterization and laser gain modeling of a NdAl3(BO3)4 (NAB) microchip laser crystal. Journal of Applied Physics, 2001, 90, 561-569.	2.5	56
84	Assessing Single Upconverting Nanoparticle Luminescence by Optical Tweezers. Nano Letters, 2015, 15, 5068-5074.	9.1	56
85	Ultrafast photochemistry produces superbright short-wave infrared dots for low-dose in vivo imaging. Nature Communications, 2020, 11, 2933.	12.8	56
86	Rareâ€Earth Spontaneous Emission Control in Threeâ€Dimensional Lithium Niobate Photonic Crystals. Advanced Materials, 2009, 21, 3526-3530.	21.0	54
87	Beyond Phototherapy: Recent Advances in Multifunctional Fluorescent Nanoparticles for Lightâ€Triggered Tumor Theranostics. Advanced Functional Materials, 2018, 28, 1803733.	14.9	54
88	Vortex lattice channeling effects in Nb films induced by anisotropic arrays of mesoscopic pinning centers. Physical Review B, 2002, 65, .	3.2	53
89	High Resolution Fluorescence Imaging of Cancers Using Lanthanide Ion-Doped Upconverting Nanocrystals. Cancers, 2012, 4, 1067-1105.	3.7	53
90	Infrared continuous-wave laser gain in neodymium aluminum borate: A promising candidate for microchip diode-pumped solid state lasers. Applied Physics Letters, 2000, 76, 2176-2178.	3.3	52

#	Article	IF	CITATIONS
91	Determining the 3D orientation of optically trapped upconverting nanorods by <i>in situ</i> single-particle polarized spectroscopy. Nanoscale, 2016, 8, 300-308.	5.6	52
92	In Vivo Deep Tissue Fluorescence and Magnetic Imaging Employing Hybrid Nanostructures. ACS Applied Materials & Interfaces, 2016, 8, 1406-1414.	8.0	52
93	Nd3+ ion based self frequency doubling solid state lasers. Optical Materials, 1999, 13, 147-157.	3.6	51
94	Femtosecond laser written surface waveguides fabricated in Nd:YAG ceramics. Optics Express, 2007, 15, 13266.	3.4	51
95	Femtosecond-laser-written, stress-induced Nd:YVO_4 waveguides preserving fluorescence and Raman gain. Optics Letters, 2010, 35, 916.	3.3	51
96	Infraredâ€Emitting Multimodal Nanostructures for Controlled In Vivo Magnetic Hyperthermia. Advanced Materials, 2021, 33, e2100077.	21.0	51
97	Continuous wave laser generation at 1064 nm in femtosecond laser inscribed Nd:YVO4 channel waveguides. Applied Physics Letters, 2010, 97, 031119.	3.3	49
98	Fluorescent nanothermometers provide controlled plasmonic-mediated intracellular hyperthermia. Nanomedicine, 2013, 8, 379-388.	3.3	49
99	Optical trapping for biosensing: materials and applications. Journal of Materials Chemistry B, 2017, 5, 9085-9101.	5.8	48
100	Spectral and thermal properties of quasiphase-matching second-harmonic-generation in Nd3+ :Sr0.6 Ba0.4 (NbO3)2 multiself-frequency-converter nonlinear crystals. Journal of Applied Physics, 2003, 93, 3111-3113.	2.5	47
101	Ultrafast laser writing of optical waveguides in ceramic Yb:YAG: a study of thermal and non-thermal regimes. Applied Physics A: Materials Science and Processing, 2011, 104, 301-309.	2.3	47
102	Phase transition in SrxBa1â^'xNb2O6ferroelectric crystals probed by Raman spectroscopy. Journal Physics D: Applied Physics, 2006, 39, 4930-4934.	2.8	46
103	Monolithic crystalline cladding microstructures for efficient light guiding and beam manipulation in passive and active regimes. Scientific Reports, 2014, 4, 5988.	3.3	46
104	Simultaneous generation of coherent light in the three fundamental colors by quasicylindrical ferroelectric domains in Sr0.6Ba0.4(NbO3)2. Applied Physics Letters, 2002, 81, 4106-4108.	3.3	45
105	Bi-functional laser and non-linear optical crystals. Optical Materials, 2006, 28, 310-323.	3.6	44
106	Spectroscopic characterisation of the Tm3+ doped KLa(WO4)2 single crystals. Optical Materials, 2006, 28, 980-987.	3.6	44
107	Ultrafast laser fabrication of low-loss waveguides in chalcogenide glass with 065  dB/cm loss. Optics Letters, 2012, 37, 1418.	3.3	44
108	Confocal Raman imaging of optical waveguides in LiNbO3 fabricated by ultrafast high-repetition rate laser-writing. Optics Express, 2008, 16, 13979.	3.4	43

#	Article	IF	CITATIONS
109	Swift nitrogen ion irradiated waveguide lasers in Nd:YAG crystal. Optics Express, 2011, 19, 5522.	3.4	42
110	Ion-implanted optical channel waveguides in neodymium-doped yttrium aluminum garnet transparent ceramics for integrated laser generation. Optics Letters, 2009, 34, 28.	3.3	41
111	Anisotropic lattice changes in femtosecond laser inscribed Nd3+:MgO:LiNbO3 optical waveguides. Journal of Applied Physics, 2009, 106, .	2.5	41
112	Time resolved spectroscopy of infrared emitting Ag ₂ S nanocrystals for subcutaneous thermometry. Nanoscale, 2017, 9, 2505-2513.	5.6	41
113	Going Above and Beyond: A Tenfold Gain in the Performance of Luminescence Thermometers Joining Multiparametric Sensing and Multiple Regression. Laser and Photonics Reviews, 2021, 15, 2100301.	8.7	41
114	Self-frequency-sum mixing in Nd doped nonlinear crystals for laser generation in the three fundamental colours. Journal of Alloys and Compounds, 2001, 323-324, 204-209.	5.5	40
115	Optical investigation of femtosecond laser induced microstress in neodymium doped lithium niobate crystals. Journal of Applied Physics, 2006, 100, 033521.	2.5	40
116	Swift heavy-ion irradiated active waveguides in Nd:YAG crystals: fabrication and laser generation. Optics Letters, 2010, 35, 3276.	3.3	40
117	Fluorescent nano-particles for multi-photon thermal sensing. Journal of Luminescence, 2013, 133, 249-253.	3.1	40
118	Continuous-wave diode-pumped Yb:glass laser with near 90% slope efficiency. Applied Physics Letters, 2006, 89, 121101.	3.3	39
119	High resolution fluorescence imaging of damage regions in H+ ion implanted Nd:MgO:LiNbO3 channel waveguides. Applied Physics Letters, 2009, 94, .	3.3	39
120	Thermally resistant waveguides fabricated in Nd:YAG ceramics by crossing femtosecond damage filaments. Optics Letters, 2010, 35, 330.	3.3	39
121	Compact, highly efficient ytterbium doped bismuthate glass waveguide laser. Optics Letters, 2012, 37, 1691.	3.3	39
122	Evaluation of ytterbium doped strontium barium niobate as a potential tunable laser crystal in the visible. Journal of Applied Physics, 2004, 95, 6185-6191.	2.5	38
123	Absorption efficiency of gold nanorods determined by quantum dot fluorescence thermometry. Applied Physics Letters, 2012, 100, 201110.	3.3	38
124	On the existence of two states in liquid water: impact on biological and nanoscopic systems. International Journal of Nanotechnology, 2016, 13, 667.	0.2	38
125	Gold nanoshells: Contrast agents for cell imaging by cardiovascular optical coherence tomography. Nano Research, 2018, 11, 676-685.	10.4	38
126	Continuous wave laser radiation at 669 nm from a self-frequency-doubled laser of YAl3(BO3)4:Nd3+. Applied Physics Letters, 1999, 74, 1788-1790.	3.3	37

#	Article	IF	CITATIONS
127	Effects of pump heating on laser and spectroscopic properties of the Nd:[YAl3(BO3)4] self-frequency-doubling laser. Journal of Applied Physics, 2000, 87, 1042-1048.	2.5	37
128	Nd3+-doped Ca3Ga2Ge3O12 garnet: A new optical pressure sensor. Journal of Applied Physics, 2013, 113, .	2.5	37
129	Subtissue Imaging and Thermal Monitoring of Cold Nanorods through Joined Encapsulation with Ndâ€Doped Infraredâ€Emitting Nanoparticles. Small, 2016, 12, 5394-5400.	10.0	37
130	Fluorescence quantum efficiency and Auger upconversion losses of the stoichiometric laser crystalNdAl3(BO3)4. Physical Review B, 2005, 72, .	3.2	36
131	Direct laser writing of near-IR step-index buried channel waveguides in rare earth doped YAG. Optics Letters, 2011, 36, 3395.	3.3	36
132	Optical Forces at the Nanoscale: Size and Electrostatic Effects. Nano Letters, 2018, 18, 602-609.	9.1	35
133	Infrared fluorescence imaging of infarcted hearts with Ag2S nanodots. Nano Research, 2019, 12, 749-757.	10.4	35
134	Self-frequency-summing NYAB laser for tunable blue generation. Optical Materials, 1999, 13, 311-317.	3.6	34
135	Spectroscopic and laser properties of Nd3+ in SBN. Journal of Luminescence, 2000, 87-89, 877-879.	3.1	34
136	Room-temperature continuous wave laser oscillations in Nd:YAG ceramic waveguides produced by carbon ion implantation. Applied Physics B: Lasers and Optics, 2011, 103, 837-840.	2.2	34
137	Reliable and Remote Monitoring of Absolute Temperature during Liver Inflammation via Luminescenceâ€Lifetimeâ€Based Nanothermometry. Advanced Materials, 2022, 34, e2107764.	21.0	34
138	Continuous-wave laser oscillation at 929nm from a Nd3+-doped LiNbO3:ZnO nonlinear laser crystal: A powerful tool for blue laser light generation. Applied Physics Letters, 2004, 85, 19-21.	3.3	33
139	Scanning confocal fluorescence imaging and micro-Raman investigations of oxygen implanted channel waveguides in Nd:MgO:LiNbO3. Applied Physics Letters, 2008, 92, .	3.3	33
140	<i>Quo Vadis</i> , Nanoparticle-Enabled <i>In Vivo</i> Fluorescence Imaging?. ACS Nano, 2021, 15, 1917-1941.	14.6	33
141	Up-conversion luminescence in the Nd3+:YAB self frequency doubling laser crystal. Optical Materials, 1998, 10, 211-217.	3.6	32
142	Order in driven vortex lattices in superconducting Nb films with nanostructured pinning potentials. Physical Review B, 2002, 65, .	3.2	32
143	Persistent luminescence nanothermometers. Applied Physics Letters, 2017, 111, .	3.3	32
144	Quantitative Comparison of the Light-to-Heat Conversion Efficiency in Nanomaterials Suitable for Photothermal Therapy. ACS Applied Materials & Interfaces, 2022, 14, 33555-33566.	8.0	32

#	Article	IF	CITATIONS
145	Continuous wave laser radiation and self-frequency-doubling in ZnO doped LiNbO3:Nd3+. Optics Communications, 1999, 161, 253-256.	2.1	31
146	High-resolution confocal fluorescence thermal imaging of tightly pumped microchip Nd:YAG laser ceramics. Applied Physics B: Lasers and Optics, 2012, 107, 697-701.	2.2	31
147	Waveguide lasers based on dielectric materials. Optical Materials, 2012, 34, 555-571.	3.6	31
148	Thulium doped LaF ₃ for nanothermometry operating over 1000 nm. Nanoscale, 2019, 11, 8864-8869.	5.6	31
149	Anisotropic pinning enhancement in Nb films with arrays of submicrometric Ni lines. Applied Physics Letters, 2002, 81, 2851-2853.	3.3	30
150	Temperature dependence of Nd3+↔Yb3+ energy transfer in the YAl3(BO3)4 nonlinear laser crystal. Journal of Applied Physics, 2005, 97, 093510.	2.5	30
151	Luminescence of lanthanide ions in strontium barium niobate. Journal of Luminescence, 2007, 122-123, 307-310.	3.1	30
152	Ion-implanted optical-stripe waveguides in neodymium-doped calcium barium niobate crystals. Optics Letters, 2009, 34, 1438.	3.3	30
153	Quantum-dot based nanothermometry in optical plasmonic recording media. Applied Physics Letters, 2014, 105, 181110.	3.3	30
154	Femtosecond laser written waveguides with MoS_2 as satuable absorber for passively Q-switched lasing. Optical Materials Express, 2016, 6, 367.	3.0	30
155	Laser gain in femtosecond microstructured Nd:MgO:LiNbO3 crystals. Applied Physics B: Lasers and Optics, 2006, 83, 559-563.	2.2	29
156	Lattice micro-modifications induced by Zn diffusion in Nd:LiNbO3 channel waveguides probed by Nd3+ confocal micro-luminescence. Applied Physics B: Lasers and Optics, 2007, 88, 201-204.	2.2	29
157	Gold nanorods for optimized photothermal therapy: the influence of irradiating in the first and second biological windows. RSC Advances, 2014, 4, 54122-54129.	3.6	29
158	Quantum Dots Emitting in the Third Biological Window as Bimodal Contrast Agents for Cardiovascular Imaging. Advanced Functional Materials, 2017, 27, 1703276.	14.9	29
159	Thermal hysteresis in the luminescence of Cr3+ ions in Sr0.6Ba0.4 (NbO3)2. Applied Physics Letters, 2004, 84, 2787-2789.	3.3	28
160	Improvement of MgF2 thin coating films for laser applications. Optical Materials, 2007, 29, 783-787.	3.6	28
161	A pump-power-controlled luminescent switcher. Applied Physics Letters, 2005, 86, 011920.	3.3	27
162	Nonlinear-laser effects in NH ₄ H ₂ PO ₄ (ADP) and ND ₄ D ₂ PO ₄ (DADP) single crystals: almost two-octave multi-wavelength Stokes and anti-Stokes combs, cascaded lasing in UV and visible ranges with the involving of the second and third harmonic generation. Laser Physics Letters, 2008, 5, 532-542.	1.4	27

#	Article	IF	CITATIONS
163	Thermal lens and heat generation of Nd:YAG lasers operating at 1.064 and 1.34 μm. Optics Express, 2008, 16, 6317.	3.4	27
164	Axial birefringence induced focus splitting in lithium niobate. Optics Express, 2009, 17, 17970.	3.4	27
165	Mirrorless buried waveguide laser in monoclinic double tungstates fabricated by a novel combination of ion milling and liquid phase epitaxy. Optics Express, 2010, 18, 26937.	3.4	27
166	Quantum dot enabled thermal imaging of optofluidic devices. Lab on A Chip, 2012, 12, 2414.	6.0	27
167	Optimum quantum dot size for highly efficient fluorescence bioimaging. Journal of Applied Physics, 2012, 111, 023513.	2.5	27
168	Optical Nanoparticles for Cardiovascular Imaging. Advanced Optical Materials, 2018, 6, 1800626.	7.3	27
169	Influence of neodymium concentration on the cw laser properties of Nd doped Ca3Ga2Ge3O12 laser garnet crystal. Journal of Applied Physics, 1999, 86, 6627-6633. <mml:math <="" td="" xmlns:mml="http://www.w3.org/1998/Math/MathML"><td>2.5</td><td>26</td></mml:math>	2.5	26
170	display="inline"> <mml:mrow><mml:msup><mml:mi mathvariant="normal">Nd<mml:mrow><mml:mn>3</mml:mn><mml:mo>+</mml:mo></mml:mrow> mathvariant="normal">Yb<mml:mrow><mml:mn>3</mml:mn><mml:mo>+</mml:mo></mml:mrow> energy transfer in the ferroelectric<mml:math <="" td="" xmlns:mml="http://www.w3.org/1998/Math/MathML"><td><td>up>smml:mo up></td></td></mml:math></mml:mi </mml:msup></mml:mrow>	<td>up>smml:mo up></td>	up>smml:mo up>
171	display="inline"> <mml:mrow><mml:msub><mml:mi .<br="" 2008,="" 77,="" b,="" mathv.="" physical="" review="">Whispering-gallery modes in glass microspheres: optimization of pumping in a modified confocal microscope. Optics Letters, 2011, 36, 615.</mml:mi></mml:msub></mml:mrow>	3.3	26
172	Switching to the brighter lane: pathways to boost the absorption of lanthanide-doped nanoparticles. Nanoscale Horizons, 2021, 6, 209-230.	8.0	26
173	New nonlinear-laser properties of ferroelectric Nd3+:Ba2NaNb5O15— cw stimulated emission (4F3/2→4I11/2and4F3/2→4I13/2), collinear and diffuse self-frequency doubling and summation. Quantum Electronics, 1999, 29, 95-97.	1.0	25
174	Microstructuration induced differences in the thermo-optical and luminescence properties of Nd:YAG fine grain ceramics and crystals. Journal of Chemical Physics, 2008, 129, 104705.	3.0	25
175	Direct laser writing of three-dimensional photonic structures in Nd:yttrium aluminum garnet laser ceramics. Applied Physics Letters, 2008, 93, 151104.	3.3	25
176	Self-frequency-doubling of ultrafast laser inscribed neodymium doped yttrium aluminum borate waveguides. Applied Physics Letters, 2011, 98, 181103.	3.3	25
177	Three-dimensional microstructuring of yttrium aluminum garnet crystals for laser active optofluidic applications. Applied Physics Letters, 2013, 103, .	3.3	25
178	The Temperature of an Optically Trapped, Rotating Microparticle. ACS Photonics, 2018, 5, 3772-3778.	6.6	25
179	Instantaneous In Vivo Imaging of Acute Myocardial Infarct by NIRâ€II Luminescent Nanodots. Small, 2020, 16, e1907171.	10.0	25
180	10-Fold Quantum Yield Improvement of Ag ₂ S Nanoparticles by Fine Compositional Tuning. ACS Applied Materials & Interfaces, 2020, 12, 12500-12509.	8.0	25

#	Article	IF	CITATIONS
181	Near infrared bioimaging and biosensing with semiconductor and rare-earth nanoparticles: recent developments in multifunctional nanomaterials. Nanoscale Advances, 2021, 3, 6310-6329.	4.6	25
182	Time resolved confocal luminescence investigations on Reverse Proton Exchange Nd:LiNbO_3 channel waveguides. Optics Express, 2007, 15, 8805.	3.4	24
183	Simultaneous dual-wavelength lasers at 1064 and 1342 nm in femtosecond-laser-written Nd:YVO_4 channel waveguides. Journal of the Optical Society of America B: Optical Physics, 2011, 28, 1607.	2.1	24
184	Improving the performance of a neodymium aluminium borate microchip laser crystal by resonant pumping. Applied Physics Letters, 2004, 85, 715-717.	3.3	23
185	Influence of Nd^3+ and Yb^3+ concentration on the Nd^3+→Yb^3+ energy-transfer efficiency in the YAL_3(BO_3)_4 nonlinear crystal: determination of optimum concentrations for laser applications. Journal of the Optical Society of America B: Optical Physics, 2004, 21, 1203.	2.1	23
186	Evaluation of rare earth doped silica sub-micrometric spheres as optically controlled temperature sensors. Journal of Applied Physics, 2012, 112, 054702.	2.5	23
187	Development and Investigation of Ultrastable PbS/CdS/ZnS Quantum Dots for Nearâ€Infrared Tumor Imaging. Particle and Particle Systems Characterization, 2017, 34, 1600242.	2.3	23
188	Cr ³⁺ based nanocrystalline luminescent thermometers operating in a temporal domain. Physical Chemistry Chemical Physics, 2020, 22, 25949-25962.	2.8	23
189	Luminescence of rare earth-doped Si–ZrO2 co-sputtered films. Journal of Luminescence, 2008, 128, 1197-1204.	3.1	22
190	Spectroscopy ofEu3+ions in congruent strontium barium niobate crystals. Physical Review B, 2008, 77,	3.2	22
191	Microstructuring of Nd:YAG crystals by proton-beam writing. Optics Letters, 2010, 35, 3898.	3.3	22
192	Single ell Biodetection by Upconverting Microspinners. Small, 2019, 15, e1904154.	10.0	22
193	Biological studies of an ICG-tagged aptamer as drug delivery system for malignant melanoma. European Journal of Pharmaceutics and Biopharmaceutics, 2020, 154, 228-235.	4.3	22
194	Exploring Single-Nanoparticle Dynamics at High Temperature by Optical Tweezers. Nano Letters, 2020, 20, 8024-8031.	9.1	22
195	Stimulated emission, excited state absorption, and laser modeling of the Nd3+:Ca3Ga2Ge3O12 laser system. Journal of Applied Physics, 2002, 91, 1754-1760.	2.5	21
196	Femtosecond-laser inscribed double-cladding waveguides in Nd:YAG crystal: a promising prototype for integrated lasers. Optics Letters, 2013, 38, 3294.	3.3	21
197	Enhancing Optical Forces on Fluorescent Upâ€Converting Nanoparticles by Surface Charge Tailoring. Small, 2015, 11, 1555-1561.	10.0	21
198	Plasmonic Copper Sulfide Nanoparticles Enable Dark Contrast in Optical Coherence Tomography. Advanced Healthcare Materials, 2020, 9, e1901627.	7.6	21

#	Article	IF	CITATIONS
199	Quantum efficiency of the self-frequency-doubling laser material. Journal of Physics Condensed Matter, 1998, 10, 7901-7905.	1.8	20
200	Continuous-wave laser properties of 4 F 3/2 ⇾ 4 I 13/2 channel in the Nd 3+ LiNbO 3 :ZnO non-linear crystal. Applied Physics B: Lasers and Optics, 2000, 70, 11-14.	2.2	20
201	Q-switched nanosecond Nd ³⁺ :Ca(NbO ₃) ₂ crystalline self-Raman laser with single-step cascade SE (l̂» _{SE} = 1.0615 <i>l̂¼<</i> m) Tj ETQq1 1 0.784314 rgBT /Overlock 10	Tf 50 667 1.4	7 Td (of <su 20</su
202	conversion. Laser Physics Letters, 2009, 6, 782-787. Multicolour second harmonic generation by strontium barium niobate nanoparticles. Journal Physics D: Applied Physics, 2009, 42, 102003.	2.8	20
203	Unveiling Molecular Changes in Water by Small Luminescent Nanoparticles. Small, 2017, 13, 1700968.	10.0	20
204	Nanojet Trapping of a Single Subâ€10Ânm Upconverting Nanoparticle in the Full Liquid Water Temperature Range. Small, 2021, 17, e2006764.	10.0	20
205	Short-pulse generation from a resonantly pumped NdAl_3(BO_3)_4 microchip laser. Optics Letters, 2005, 30, 397.	3.3	19
206	Passive Q-switching of a diode pumped Nd3+:CGGG crystal: Benefits of inhomogeneous line broadening and short pulse generation. Optical Materials, 2006, 28, 408-414.	3.6	19
207	Lanthanide doped strontium barium niobate: Optical spectroscopy and local structure at the impurity sites. Journal of Alloys and Compounds, 2008, 451, 12-17.	5.5	19
208	Femtosecond laser writing of multifunctional optical waveguides in a Nd:YVO_4+KTP hybrid system. Optics Letters, 2011, 36, 975.	3.3	19
209	Dynamic single gold nanoparticle visualization by clinical intracoronary optical coherence tomography. Journal of Biophotonics, 2017, 10, 674-682.	2.3	19
210	Hyperspectral Imaging and Optical Trapping: Complementary Tools for Assessing Directionâ€Dependent Polarized Emission from Single Upconverting LiYF ₄ :Yb ³⁺ /Er ³⁺ Microparticles. Advanced Optical Materials, 2021, 9, 2100101.	7.3	19
211	Dielectric anomalous response of water at 60°C. Philosophical Magazine, 2015, 95, 683-690.	1.6	18
212	Femtosecond Laser Writing of Optical Waveguides by Self-Induced Multiple Refocusing in LiTaO ₃ Crystal. Journal of Lightwave Technology, 2019, 37, 3452-3458.	4.6	18
213	Nanopatterning effects on magnetic anisotropy of epitaxial Fe(001) micrometric squares. Journal of Applied Physics, 2002, 91, 382.	2.5	17
214	Simulations and experiments on magneto-optical diffraction by an array of epitaxial Fe(001) microsquares. Applied Physics Letters, 2002, 81, 3206-3208.	3.3	17
215	Optical properties of single doped Cr3+ and co-doped Cr3+–Nd3+ aluminum tantalum tellurite glasses. Journal of Alloys and Compounds, 2004, 380, 163-166.	5.5	17
216	High repetition rate UV ultrafast laser inscription of buried channel waveguides in Sapphire: Fabrication and fluorescence imaging via ruby R lines. Optics Express, 2009, 17, 10076.	3.4	17

#	Article	IF	CITATIONS
217	Thermal stability of microstructural and optical modifications induced in sapphire by ultrafast laser filamentation. Journal of Applied Physics, 2010, 107, .	2.5	17
218	Non-linear niobate nanocrystals for two-photon imaging. Optical Materials, 2011, 33, 258-266.	3.6	17
219	Invited Article: Experimental evaluation of gold nanoparticles as infrared scatterers for advanced cardiovascular optical imaging. APL Photonics, 2018, 3, .	5.7	17
220	Spectroscopic study of Y b3+centres in the Y Al3(BO3)4nonlinear laser crystal. Journal of Physics Condensed Matter, 2003, 15, 7789-7801.	1.8	16
221	Bistable chromatic switching inYb3+-dopedNdPO4crystals. Physical Review B, 2006, 74, .	3.2	16
222	Second harmonic and Raman imaging of He^+ implanted KTiOPO_4 waveguides. Optics Express, 2011, 19, 13934.	3.4	16
223	Thermal loading in flow-through electroporation microfluidic devices. Lab on A Chip, 2013, 13, 3119-3127.	6.0	16
224	Optical lattice-like cladding waveguides by direct laser writing: fabrication, luminescence, and lasing. Optics Letters, 2016, 41, 2169.	3.3	16
225	Magnetic Nanoplatelets for High Contrast Cardiovascular Imaging by Magnetically Modulated Optical Coherence Tomography. ChemPhotoChem, 2019, 3, 529-539.	3.0	16
226	Boosting the Near-Infrared Emission of Ag ₂ S Nanoparticles by a Controllable Surface Treatment for Bioimaging Applications. ACS Applied Materials & Interfaces, 2022, 14, 4871-4881.	8.0	16
227	Cr3+→Nd3+ energy transfer in the YAl3(BO3)4 nonlinear laser crystal. Journal of Applied Physics, 2005, 98, 023103.	2.5	15
228	Carbon ion implanted Nd:MgO:LiNbO_3 optical channel waveguides: an intermediate step between light and heavy ion implanted waveguides. Optics Express, 2010, 18, 5951.	3.4	15
229	Upconversion emission obtained in Yb^3+-Er^3+ doped fluoroindate glasses using silica microspheres as focusing lens. Optics Express, 2013, 21, 10667.	3.4	15
230	Synthesis and characterization of Ag ₂ S and Ag ₂ S/Ag ₂ (S,Se) NIR nanocrystals. Nanoscale, 2019, 11, 9194-9200.	5.6	15
231	Autofluorescence-Free <i>In Vivo</i> Imaging Using Polymer-Stabilized Nd ³⁺ -Doped YAG Nanocrystals. ACS Applied Materials & Interfaces, 2020, 12, 51273-51284.	8.0	15
232	Red, blue, and green laser-light generation from the NYAB nonlinear crystal. Optical Engineering, 1999, 38, 1794.	1.0	14
233	Mixed-state properties of superconducting Nb/Ni superlattices. Physica C: Superconductivity and Its Applications, 2002, 369, 213-216.	1.2	14
234	Thermal lens spectroscopy through phase transition in neodymium doped strontium barium niobate laser crystals. Journal of Applied Physics, 2007, 101, 023113.	2.5	14

#	Article	IF	CITATIONS
235	Laser action from Yb3+ ions in the ferroelectric and paraelectric phases of strontium barium niobate. Applied Physics Letters, 2008, 92, .	3.3	14
236	The effect of Nd and Mg doping on the micro-Raman spectra of LiNbO ₃ single-crystals. Journal of Physics Condensed Matter, 2009, 21, 145401.	1.8	14
237	A zero-field single-molecule magnet with luminescence thermometry capabilities containing soft donors. Journal of Materials Chemistry C, 2022, 10, 13946-13953.	5.5	14
238	Up-conversion luminescence in the Ca3Ga2Ge3O12:Nd3+laser garnet crystal. Journal of Physics Condensed Matter, 2000, 12, L441-L449.	1.8	13
239	Spectroscopic and laser gain properties of the Nd3+:β'-Gd2(MoO4)3non-linear crystal. Journal of Physics Condensed Matter, 2000, 12, 9699-9714.	1.8	13
240	TunableNd3+:Ca3Ga2Ge3O12site-selective laser operating around 1.33 μm. Physical Review B, 2004, 70, .	3.2	13
241	Up-conversion luminescence in the NdAl3(BO3)4 (NAB) microchip laser crystal. Optical Materials, 2004, 25, 9-15.	3.6	13
242	Luminescence of Rare Earth Ions in Strontium Barium Niobate Around the Phase Transition: The Case of Tm3 + Ions. Ferroelectrics, 2008, 363, 150-162.	0.6	13
243	NIR fluorescence quenching by OH acceptors in the Nd 3+ doped KY 3 F 10 nanoparticles synthesized by microwave-hydrothermal treatment. Journal of Alloys and Compounds, 2016, 661, 312-321.	5.5	13
244	Lightâ€Activated Upconverting Spinners. Advanced Optical Materials, 2018, 6, 1800161.	7.3	13
245	Effect of H2O and D2O Thermal Anomalies on the Luminescence of Eu3+ Aqueous Complexes. Journal of Physical Chemistry C, 2018, 122, 14838-14845.	3.1	13
246	Reaching Deeper: Absolute In Vivo Thermal Reading of Liver by Combining Superbright Ag ₂ S Nanothermometers and In Silico Simulations. Advanced Science, 2021, 8, 2003838.	11.2	13
247	First observations of stimulated emission and of stimulated Raman scattering in acentric cubic Nd3+:Bi12SiO20crystals. Quantum Electronics, 1999, 29, 6-8.	1.0	12
248	74% Slope efficiency from a diode-pumped Yb3+:LiNbO3:MgO laser crystal. Applied Physics B: Lasers and Optics, 2003, 77, 621-623.	2.2	12
249	Single longitudinal mode laser oscillation from a neodymium aluminium borate stoichiometric crystal. Applied Physics Letters, 2005, 87, 211108.	3.3	12
250	Self-activated Nd3+:Ba2NaNb5O12 optical super-lattices: Micro characterization and non-collinear laser light generation. Optics Communications, 2006, 262, 220-223.	2.1	12
251	Time-resolved study electronic and thermal contributions to the nonlinear refractive index of Nd3+:SBN laser crystals. Journal of Luminescence, 2008, 128, 1013-1015.	3.1	12
252	Investigation of neodymium-diffused yttrium vanadate waveguides by confocal microluminescence. Journal of Applied Physics, 2008, 103, .	2.5	12

#	Article	IF	CITATIONS
253	Optical channel waveguides in Nd:LGS laser crystals produced by proton implantation. Optics Express, 2010, 18, 16258.	3.4	12
254	Flow effects in the laser-induced thermal loading of optical traps and optofluidic devices. Optics Express, 2014, 22, 23938.	3.4	12
255	Upconverting Nanorockers for Intracellular Viscosity Measurements During Chemotherapy. Advanced Biology, 2019, 3, e1900082.	3.0	12
256	High-pressure luminescence in Nd3+-doped MgO:LiNbO3. High Pressure Research, 2006, 26, 341-344.	1.2	11
257	Energy transfer processes in the ytterbium doped NdPO4 stoichiometric crystal. Optical Materials, 2006, 28, 1280-1283.	3.6	11
258	Dielectric anomalies in Nd3+ doped Ba2NaNb5O15 laser crystal. Journal of Alloys and Compounds, 2008, 451, 198-200.	5.5	11
259	Nonlinear refraction and absorption through phase transition in a Nd:SBN laser crystal. Physical Review B, 2009, 79, .	3.2	11
260	Characterization of active waveguides fabricated by ultralow-fluence swift heavy ion irradiation in lithium niobate crystals. Journal Physics D: Applied Physics, 2011, 44, 105103.	2.8	11
261	Two-photon luminescence thermometry: towards 3D high-resolution thermal imaging of waveguides. Optics Express, 2016, 24, 16156.	3.4	11
262	Continuous wave laser radiation at 693 nm from LiNbO 3 :ZnO:Nd 3+ nonlinear laser crystal. Applied Physics B: Lasers and Optics, 2000, 70, 483-486.	2.2	10
263	Continuous wave ultraviolet laser source based on self-frequency-sum-mixing in Nd3+:YAl3(BO3)4 nonlinear laser crystal. Journal of Applied Physics, 2001, 90, 1070-1072.	2.5	10
264	field optical and micro-luminescence investigations of femtosecond laser micro-structured Nd:YAG crystals. Optics Express, 2007, 15, 3285.	3.4	10
265	Active waveguide in Nd3+:MgO:LiNbO3 crystal produced by low-dose carbon ion implantation. Applied Physics Letters, 2008, 92, 021110.	3.3	10
266	Low-dose O ³⁺ ion-implanted active optical planar waveguides in Nd : YAG crystals: guiding properties and micro-luminescence characterization. Journal Physics D: Applied Physics, 2008, 41, 175112.	2.8	10
267	Microstructural imaging of high repetition rate ultrafast laser written LiTaO3 waveguides. Applied Physics Letters, 2009, 94, 081106.	3.3	10
268	Ultrafast laser inscription of bistable and reversible waveguides in strontium barium niobate crystals. Applied Physics Letters, 2010, 96, .	3.3	10
269	μ-Raman spectroscopy characterization of LiNbO3femtosecond laser written waveguides. Journal of Applied Physics, 2012, 112, 123108.	2.5	10
270	Second harmonic generation of violet light in femtosecond-laser-inscribed BiB_3O_6 cladding waveguides. Optical Materials Express, 2013, 3, 1279.	3.0	10

#	Article	IF	CITATIONS
271	Compositional Tuning of Light-to-Heat Conversion Efficiency and of Optical Properties of Superparamagnetic Iron Oxide Nanoparticles. Journal of Physical Chemistry C, 2018, 122, 16389-16396.	3.1	10
272	Lanthanide doped nanoheaters with reliable and absolute temperature feedback. Physica B: Condensed Matter, 2022, 631, 413652.	2.7	10
273	Quantum efficiency of Nd-doped lasers measured by pump-induced crystal heating: application to the Nd3+:Gd2(MoO4)3 crystal. Applied Physics B: Lasers and Optics, 2001, 72, 811-814.	2.2	9
274	Intracavity second harmonic generation in the green from a diode-end-pumped Nd3+:Ca3Ga2Ge3O12 laser garnet crystal. Journal of Applied Physics, 2002, 92, 3436-3441.	2.5	9
275	Optical distortions through phase transition in the Nd3+:SBN laser crystal. Applied Physics Letters, 2006, 88, 161116.	3.3	9
276	Effects of neodymium incorporation on the structural and luminescence properties of the YAl3(BO3)4–NdAl3(BO3)4system. Journal of Physics Condensed Matter, 2007, 19, 246204.	1.8	9
277	Optical spectra of Tm3+-doped YAl3(BO3)4 single crystals. Physica Status Solidi C: Current Topics in Solid State Physics, 2007, 4, 809-812.	0.8	9
278	Desvitrification on an oxyfluoride glass doped with Tm3+ and Yb3+ ions under Ar laser irradiation. Journal of Luminescence, 2008, 128, 905-907.	3.1	9
279	Origin of the refractive index modification of femtosecond laser processed doped phosphate glass. Journal of Applied Physics, 2011, 109, .	2.5	9
280	Core–Shell Engineering to Enhance the Spectral Stability of Heterogeneous Luminescent Nanofluids. Particle and Particle Systems Characterization, 2017, 34, 1700276.	2.3	9
281	pH dependence of water anomaly temperature investigated by Eu(III) cryptate luminescence. Analytical and Bioanalytical Chemistry, 2020, 412, 73-80.	3.7	9
282	The nearâ€infrared autofluorescence fingerprint of the brain. Journal of Biophotonics, 2020, 13, e202000154.	2.3	9
283	Continuous wave laser radiation at 1314 and 1386 nm and infrared to red self-frequency doubling in nonlinear LaBGeO5:Nd3+ crystal. Applied Physics Letters, 1999, 75, 2722-2724.	3.3	8
284	Tunable green laser source based on frequency mixing of pump and laser radiation from a Nd:YVO_4 crystal operating at 1342 nm with an intracavity KTP crystal. Applied Optics, 2002, 41, 6394.	2.1	8
285	Photo-luminescence studies of strontium barium niobate crystals doped with Cr3+ ions. Chemical Physics Letters, 2006, 417, 196-199.	2.6	8
286	Near-field imaging of femtosecond laser ablated sub-λ/4 holes in lithium niobate. Applied Physics Letters, 2009, 95, 181103.	3.3	8
287	Response to "Critical Growth Temperature of Aqueous CdTe Quantum Dots is Nonâ€negligible for their Application as Nanothermometers†Small, 2013, 9, 3198-3200.	10.0	8
288	A 2D μ-Raman analysis of low repetition rate femto-waveguides in lithium niobate by using a finite element model. Optical Materials, 2014, 36, 936-940.	3.6	8

#	Article	IF	CITATIONS
289	Plug and Play Anisotropy-Based Nanothermometers. ACS Photonics, 2018, 5, 2676-2681.	6.6	8
290	Multichannel Fluorescence Microscopy: Advantages of Going beyond a Single Emission. Advanced NanoBiomed Research, 2022, 2, .	3.6	8
291	Ferroelectric Nd3+:SrxBa1-x(NbO3)2—a new nonlinear laser crystal: cw 1-μm stimulated emission (4F3/2→4I11/2) and diffuse self-frequency doubling. Quantum Electronics, 1998, 28, 1031-1033.	1.0	7
292	Optical spectroscopy of in the piezoelectric crystal. Journal of Physics Condensed Matter, 1999, 11, 3201-3207.	1.8	7
293	Oxygen content influence in the superconducting and electronic properties of Nd1.85Ce0.15Cu1.01Oy ceramics. Journal of Alloys and Compounds, 2001, 323-324, 580-583.	5.5	7
294	Simultaneous generation of coherent light in the red, green and blue from Nd3+ doped non-linear crystals. Optical Materials, 2003, 24, 411-417.	3.6	7
295	Excited-state absorption in NdAl3(BO3)4 laser crystal. Applied Physics Letters, 2003, 82, 3826-3828.	3.3	7
296	Femtosecond laser induced micromodifications in Nd:SBN crystals: Amorphization and luminescence inhibition. Journal of Applied Physics, 2006, 100, 113517.	2.5	7
297	Luminescence life time and time-resolved spectroscopy of Cr3+ ions in strontium barium niobate. Journal of Luminescence, 2006, 119-120, 453-456.	3.1	7
298	Optical channel waveguide in Nd/Ce codoped YAG laser crystal produced by carbon ion implantation. Applied Optics, 2009, 48, 4514.	2.1	7
299	Luminescence Quantum Efficiency of \${m Nd}^{3+}{colon}{m Y}_{3}{m Al}_{5}{m O}_{12}\$ Garnet Laser Ceramics Determined by Pump-Induced Line Broadening. IEEE Journal of Quantum Electronics, 2010, 46, 1870-1876.	1.9	7
300	Thermal optimization and erasing of Nd:YAG proton beam written waveguides. Optics Letters, 2011, 36, 3278.	3.3	7
301	Gold nanorod assisted intracellular optical manipulation of silica microspheres. Optics Express, 2014, 22, 19735.	3.4	7
302	Thermo-optical and spectroscopic properties of Nd:YAG fine grain ceramics: towards a better performance than the Nd:YAG laser crystals. Laser Physics Letters, 2016, 13, 025004.	1.4	7
303	Laser Refrigeration by an Ytterbiumâ€Doped NaYF ₄ Microspinner. Small, 2021, 17, e2103122.	10.0	7
304	Investigation of the concentration- and temperature-dependent motion of colloidal nanoparticles. Nanoscale, 2020, 12, 12561-12567.	5.6	7
305	Multiphoton imaging of melanoma 3D models with plasmonic nanocapsules. Acta Biomaterialia, 2022, 142, 308-319.	8.3	7
306	Luminescence Thermometry for Brain Activity Monitoring: A Perspective. Frontiers in Chemistry, 0, 10, .	3.6	7

#	Article	IF	CITATIONS
307	CW end-pumped Nd3+:LaBGeO5 mini laser for self-frequency-doubling. Journal of Luminescence, 1997, 72-74, 816-818.	3.1	6
308	Temperature decrease induced by stimulated emission in the Nd3+ ion-doped YAl3(BO3)4 crystal. Chemical Physics Letters, 2001, 334, 309-313.	2.6	6
309	Interplay between the vortex lattice and arrays of submicrometric pinning centers. Physica C: Superconductivity and Its Applications, 2002, 369, 135-140.	1.2	6
310	Site-selective study of Nd3+ optical centers in Ca3Sc2Ge3O12 laser garnet crystals. Journal of Applied Physics, 2004, 95, 1774-1779.	2.5	6
311	Localized desvitrifiation in Er3+-doped strontium barium niobate glass by laser irradiation. Applied Physics A: Materials Science and Processing, 2008, 93, 977-981.	2.3	6
312	Effects of laser light confinement in periodically poled orthorhombic non-centrosymmetric Ba2NaNb5O15crystals. Laser Physics Letters, 2008, 5, 291-295.	1.4	6
313	Ionoluminescence of trivalent rare-earth-doped strontium barium niobate. Journal of Luminescence, 2008, 128, 735-737.	3.1	6
314	Optical spectroscopy of neodymium-doped calcium barium niobate ferroelectric crystals. Journal of Luminescence, 2009, 129, 1658-1660.	3.1	6
315	Fluorescence-Quenching Free Channel Waveguides in Yb:YAG Ceramics by Carbon Ion Implantation. Journal of Lightwave Technology, 2011, 29, 1460-1464.	4.6	6
316	Microspectroscopy of ultrafast laser inscribed channel waveguides in Yb:tungstate crystals. Applied Physics Letters, 2011, 98, 141108.	3.3	6
317	Molecular Imaging of Infarcted Heart by Biofunctionalized Gold Nanoshells. Advanced Healthcare Materials, 2021, 10, e2002186.	7.6	6
318	In Vivo Nearâ€Infrared Imaging Using Ternary Selenide Semiconductor Nanoparticles with an Uncommon Crystal Structure. Small, 2021, 17, e2103505.	10.0	6
319	Electrospraying as a Technique for the Controlled Synthesis of Biocompatible PLGA@Ag2S and PLGA@Ag2S@SPION Nanocarriers with Drug Release Capability. Pharmaceutics, 2022, 14, 214.	4.5	6
320	Piezoelectric Sillenite Bi12SiO20:Nd3+. A New Laser and SRS-Active Crystal. Physica Status Solidi (B): Basic Research, 1998, 210, R9-R10.	1.5	5
321	Solid state laser source for simultaneous generation of green and red radiation. Journal Physics D: Applied Physics, 2002, 35, 2711-2715.	2.8	5
322	Optimum conditions for ultraviolet-laser generation based on self-frequency sum mixing in Nd^3+-activated borate crystals. Journal of the Optical Society of America B: Optical Physics, 2002, 19, 1326.	2.1	5
323	Diode-pumped laser action at 134 µm from the Nd^3+: Ca_3Ga_2Ge_3O_12 garnet crystal: influence of Nd^3+ multicenter distribution. Journal of the Optical Society of America B: Optical Physics, 2003, 20, 2075.	2.1	5
324	Rare Earth Ion Doped Non Linear Laser Crystals. Radiation Effects and Defects in Solids, 2003, 158, 231-239.	1.2	5

#	Article	IF	CITATIONS
325	Ultraviolet nanosecond laser-assisted micro-modifications in lithium niobate monitored by Nd3+ luminescence. Applied Physics A: Materials Science and Processing, 2007, 87, 87-90.	2.3	5
326	Photoluminescence of Er-doped Si-SiO2 and Al–Si-SiO2 sputtered thin films. Journal of Luminescence, 2008, 128, 897-900.	3.1	5
327	Heat in optical tweezers. Proceedings of SPIE, 2013, , .	0.8	5
328	Excited state absorption of pump and laser radiations in NYAB non-linear crystal operating at 1.3µm for visible laser light generation. EPJ Applied Physics, 2000, 10, 29-32.	0.7	5
329	Clickable Albumin Nanoparticles for Pretargeted Drug Delivery toward PD-L1 Overexpressing Tumors in Combination Immunotherapy. Bioconjugate Chemistry, 2022, , .	3.6	5
330	Fluorescence dynamics and laser properties of the Nd3+:Ca3Ga2Ge3O12 crystal. Journal of Luminescence, 1999, 83-84, 477-479.	3.1	4
331	Concentration effect on the up-conversion luminescence of neodymium activated calcium gallium germanium garnet crystal. Journal of Alloys and Compounds, 2001, 323-324, 312-314.	5.5	4
332	Optical Properties of Active Ions Around the Ferro-Paraelectric Phase Transition in SBN Crystals. Ferroelectrics, 2006, 337, 33-39.	0.6	4
333	Wide infrared and visible tunability from a Nd3+:Ba2NaNbO15 self-frequency-converter disordered laser crystal. Journal of Applied Physics, 2006, 99, 026105.	2.5	4
334	Improvement of laser gain by microdomain compensation effects in Nd:SrBa(Nb3O)2 lasers. Journal of Applied Physics, 2007, 102, 053101.	2.5	4
335	Confocal Luminescence Investigations of Two-Beam Direct-UV-Written Silica-On-Silicon Waveguides. IEEE Journal of Quantum Electronics, 2008, 44, 1219-1224.	1.9	4
336	Suppression of Q-switching instabilities in a passively mode-locked Nd:Y3Al5O12 ceramic laser. Optical Materials, 2009, 31, 725-728.	3.6	4
337	Luminescence of Er-doped silicon oxide–zirconia thin films. Journal of Luminescence, 2009, 129, 696-703.	3.1	4
338	The effect of the ferroelectric domain walls in the scanning near field optical microscopy response of periodically poled Ba2NaNb5O15and LiNbO3crystals. Journal of Physics Condensed Matter, 2009, 21, 042201.	1.8	4
339	Nanoprobes for Biomedical Imaging with Tunable Nearâ€Infrared Optical Properties Obtained via Green Synthesis. Advanced Photonics Research, 0, , 2100260.	3.6	4
340	Bismuth Selenide Nanostructured Clusters as Optical Coherence Tomography Contrast Agents: Beyond Gold-Based Particles. ACS Photonics, 2022, 9, 559-566.	6.6	4
341	Hall effect in Nd1.85Ce0.15CuOy with controlled oxygen content. Physica C: Superconductivity and Its Applications, 2000, 341-348, 1943-1944.	1.2	3
342	Spectroscopy and Continuous Wave Near-Infrared Stimulated Emission of New Yttrium Gallium Garnet {Y3}[Y, Ga](Ga3)O12:Nd3+ (YGaO3:Nd3+). Optical Review, 2000, 7, 101-111.	2.0	3

#	Article	IF	CITATIONS
343	A new crystalline host for lasing Ln3+ ions: disordered calcium–lutetium fluoride. Journal of Alloys and Compounds, 2001, 323-324, 376-379.	5.5	3
344	Fabrication of 2D, 1D and 0D ordered metallic nanostructures. Vacuum, 2002, 67, 693-698.	3.5	3
345	Intracavity thermal loading measurements and evaluation of the intrinsic fluorescence quantum efficiency in Yb3+:LiNbO3:MgO lasers. Applied Physics Letters, 2006, 89, 091122.	3.3	3
346	Lowâ€dose ion implanted active waveguides in Nd ³⁺ doped nearâ€stoichiometric lithium niobate: promising candidates for near infrared integrated laser. Physica Status Solidi - Rapid Research Letters, 2008, 2, 141-143.	2.4	3
347	Periodic Ferroelectric Domain Structures Characterization by Scanning Near Field Optical Microscopy. Ferroelectrics, 2008, 363, 187-198.	0.6	3
348	Enhanced Second Harmonic Generation in Femtosecond Laser Inscribed Double-Cladding Waveguide of Nd:GdCOB Crystal. Journal of Lightwave Technology, 2013, 31, 3873-3878.	4.6	3
349	Simultaneous generation of violet, blue, and green lasers using Nd:YAl ₃ (BO ₃) ₄ channel waveguides under pumping at 815 nm. Physica Status Solidi - Rapid Research Letters, 2013, 7, 1018-1021.	2.4	3
350	Stress-induced waveguides in Nd:YAG by simultaneous double-beam irradiation with femtosecond pulses. Optical Materials, 2016, 51, 84-88.	3.6	3
351	New opportunities for light-based tumor treatment with an "iron fist― Light: Science and Applications, 2022, 11, 65.	16.6	3
352	Bi5.8PO11.2 : Nd3+ — a New Bismuth-Containing Laser Crystal. Physica Status Solidi A, 1999, 175, R9-R10.	1.7	2
353	Thermal loading in highly efficient diode pumped ytterbium doped lithium niobate lasers. , 0, , .		2
354	Dependence of the Refractive Indices in LiNbO ₃ :Cr Crystals Doped with HfO ₂ . Materials Science Forum, 2005, 480-481, 423-428.	0.3	2
355	BPM simulation of SNOM measurements of waveguide arrays induced by periodically poled BNN crystals. Optical and Quantum Electronics, 2007, 39, 805-811.	3.3	2
356	Near-field-optical-microscopy studies of micro-modifications caused by femtosecond laser irradiation in lithium niobate crystals. Applied Physics A: Materials Science and Processing, 2008, 93, 177-181.	2.3	2
357	Confocal micro-luminescence of Zn-diffused LiNbO3:Tm3+ channel waveguides. Journal of Luminescence, 2009, 129, 1698-1701.	3.1	2
358	Strong ion migration in high refractive index contrast waveguides formed by femtosecond laser pulses in phosphate glass. , 2014, , .		2
359	New strategies for luminescence thermometry in the biological range using upconverting nanoparticles. , 2014, , .		2
360	Eu3+ luminescent ions detect water density anomaly. Journal of Luminescence, 2020, 223, 117263.	3.1	2

#	Article	IF	CITATIONS
361	Avoiding induced heating in optical trap. , 2017, , .		2
362	Optical detection of atherosclerosis at molecular level by optical coherence tomography: An in vitro study. Nanomedicine: Nanotechnology, Biology, and Medicine, 2022, 43, 102556.	3.3	2
363	Red-, blue-, and green-laser-light generation from the NYAB nonlinear crystal. , 1999, , .		1
364	New Laser Garnet Crystal with Disordered Structure. Japanese Journal of Applied Physics, 1999, 38, L1180-L1182.	1.5	1
365	New Nd3+:CaLu2F8laser crystal containing lutetium. Quantum Electronics, 1999, 29, 375-377.	1.0	1
366	Cr ³⁺ ions location in codoped LiNbO ₃ :Sc ₂ o ₃ crystals. Radiation Effects and Defects in Solids, 2001, 155, 235-239.	1.2	1
367	Codoping Effects on the Laser Gain of Neodymium Activated Lithium Niobate Crystals. Ferroelectrics, 2002, 273, 193-198.	0.6	1
368	Determination of magnetic axes distribution in epitaxial Fe (001) micrometric squares by magneto optical technique. Journal of Magnetism and Magnetic Materials, 2002, 240, 37-39.	2.3	1
369	Bistable luminescence of trivalent rare-earth ions in crystals. Journal of Luminescence, 2006, 119-120, 314-317.	3.1	1
370	Phase transition induced gain depression in Nd[sup 3+]:SBN lasers. Journal of Applied Physics, 2006, 100, 113114.	2.5	1
371	Growth of Nanocrystals in a Nd ³⁺ –Yb ³⁺ Codoped Oxyfluoride Glass by Laser Irradiation. Journal of Nanoscience and Nanotechnology, 2009, 9, 3771-3774.	0.9	1
372	Control of the local devitrification on oxyfluoride glass doped with Er3+ ions under diode laser irradiation. Journal of Applied Physics, 2010, 108, 103103.	2.5	1
373	Near-field local enhancement by ordered arrays of sub-wavelength scattering centers fabricated by femtosecond ablation. Applied Physics B: Lasers and Optics, 2011, 103, 51-55.	2.2	1
374	Study of the refractive index modification mechanisms of femtosecond laser processed waveguides in doped phosphate glass through its micro photoluminescence properties. , 2011, , .		1
375	3D microfabrication in YAG crystals by direct laser writing and chemical etching. , 2013, , .		1
376	All-optical thermal microscopy of laser-excited waveguides. Optics Letters, 2016, 41, 2061.	3.3	1
377	Facile and fast synthesis of lanthanide nanoparticles for bio-applications. , 2020, , 195-228.		1
378	Micro-luminescence and Micro-Raman Mapping of Ultrafast Laser Inscribed Yb:KGd(WO4)2 and Yb:KY(WO4)2 Channel Waveguides. , 2010, , .		1

#	Article	IF	CITATIONS
379	Quantum dot thermal imaging of on-chip laser excited microfluidics. , 2012, , .		1
380	Microrheometric upconversion-based techniques for intracellular viscosity measurements. , 2017, , .		1
381	Recent developments in Nd/sup 3+/:Ba/sub 2/NaNb/sub 5/O/sub 15/ non linear lasers: Tuneability and non collinear intracavity propagation. , 0, , .		0
382	Heat generation with and without laser operation (at 1064 and 1340 nm) in Nd:YAC. , 2006, , .		0
383	Application of near field optical microscopy to the study of femtosecond laser micro-structured Nd:YAG crystals. , 2007, , .		0
384	Damage channeling in femtosecond laser micro-structured SBN crystals. Applied Surface Science, 2008, 255, 3132-3136.	6.1	0
385	Ultrafast laser fabrication of 3D waveguides in sapphire. , 2009, , .		0
386	Influence of Pulse Width in Ultrafast Laser Fabrication of Embedded Waveguides in Chalcognide Glasses. , 2011, , .		0
387	Double-Filament Waveguides Written in Nd:YAG Ceramic With 2-ps UV Laser Pulses. , 2011, , .		0
388	Photoluminescence of Er-doped silicon-rich oxide thin films with high Al concentrations. Physics Procedia, 2011, 13, 54-57.	1.2	0
389	Continuous flow single cell electroporation in an ultrafast laser inscribed optofluidic device. , 2012, , .		0
390	Ultrafast Laser Fabrication of Low-Loss Waveguides in Chalcogenide Glass with 0.65 dB/cm Loss. , 2012, , .		0
391	Second Harmonic Generation of Violet Light in Femtosecond-Laser-Inscribed BiB3O6Cladding Waveguides. MATEC Web of Conferences, 2013, 8, 06011.	0.2	0
392	Femtosecond-laser inscription via local modification of the glass composition in phosphate glasses. , 2014, , .		0
393	Fluorescence imaging of lattice re-distribution on step-index direct laser written Nd:YAG waveguide lasers. Journal of Applied Physics, 2015, 117, 023112.	2.5	0
394	On the change of paraelectric behavior of water at T = T* = 60 °C as a polar liquid. Ferro 533, 108-114.	electrics, 2	2018,
395	Magnetic Nanoplatelets for High Contrast Cardiovascular Imaging by Magnetically Modulated Optical Coherence Tomography. ChemPhotoChem, 2019, 3, 503-503.	3.0	0

Second harmonic and Raman imaging of ultrafast laser written LiTaO3 waveguides. , 2009, , .

0

#	Article	IF	CITATIONS
397	Highly Efficient Waveguide Lasers in a Femtosecond Laser Inscribed Nd:YVO4 Channel Waveguide. , 2011, , .		0
398	Codoping Effects on the Laser Gain of Neodymium Activated Lithium Niobate Crystals. Ferroelectrics, 2002, 273, 193-198.	0.6	0